Supplementary Materials

Characterization of interconnectivity of gelatin methacrylate hydrogels using photoacoustic imaging

Wenxiu Zhao,[a,b,c] Haibo Yu,[a,b*] Zhixing Ge,[a,b,c] Xiaoduo Wang,[a,b] Yuzhao Zhang,[a,b,c]

Yangdong Wen,[d] Hao Luo,[a,b,c] Lianqing Liu,[a,b] and Wen Jung Li [a,b,e*]

[a.]State Key Laboratory of Robotics, Shenyang Institute of Automation, Chinese Academy of Sciences, Shenyang 110016, China

[b.]Institutes for Robotics and Intelligent Manufacturing, Chinese Academy of Sciences, Shenyang 110016, China

[c.]University of Chinese Academy of Sciences, Beijing 100049, China

[d.]Institute of Urban Rail Transportation, Southwest Jiaotong University, Chengdu 610000, China

[e.]Department of Mechanical Engineering, City University of Hong Kong, Hong Kong SAR, China

[*] Corresponding authors; e-mail: yuhaibo@sia.cn, wenjli@cityu.edu.hk

This file includes:

Fig. S1 to S4.

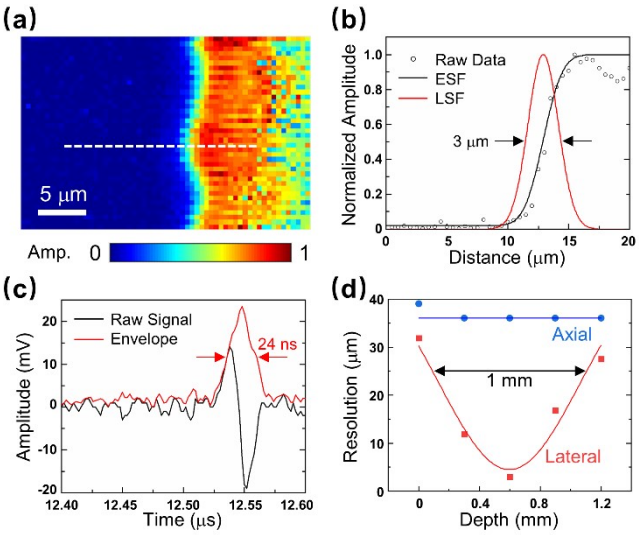

Fig. S1. (a) PA image of the edge of a sharp metallic blade at the depth of 0.6 mm. (b) PA signals along the white dash line in (a), the error spread function (ESF) which was fitted based on the raw PA data, and the line spread function (LSF) which was calculated from the derivation of ESF. The full width at half maximum (FWHM) of LSF was measured to represent the lateral resolution. (c) A PA signal of the blade measured at the depth of 0.6 mm; Hilbert transformation was applied to the PA signal to get its envelope. The FWHM of the envelope was measured to represent the axial resolution. Since water is used as the medium, the axial resolution of the system could be estimated as 36 μm considering the ultrasound speed as 1500 m/s in the medium. (d) The lateral and axial resolutions measured at different depths.

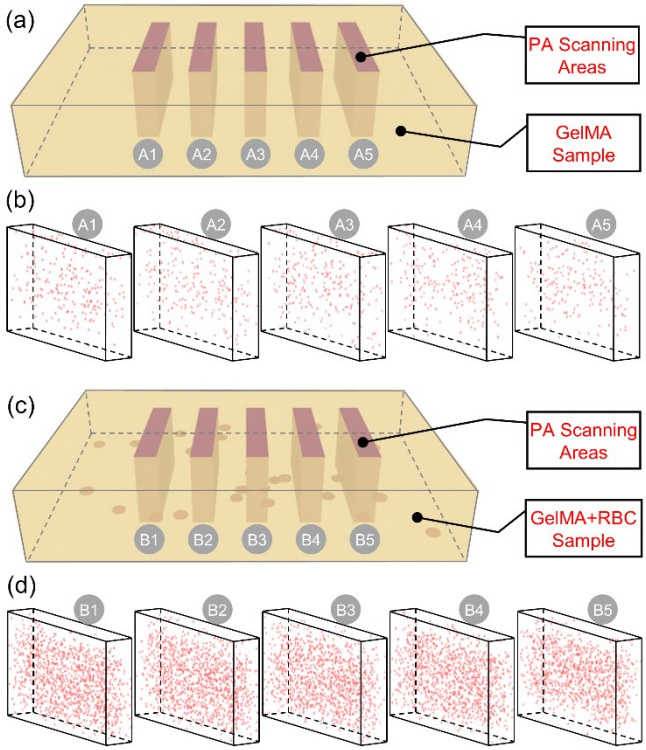

Fig. S2. (a) is the diagram of PA scanning of the GelMA sample without RBCs. Five volumes were scanned and the corresponding PA images are shown in (b). (c) is the diagram of PA scanning of the GelMA sample with RBCs. Five volumes were scanned and the corresponding PA images are shown in (d). The GelMA samples in (a) and (c) were with the thickness of 0.55 mm. A1 in (b) is showing the same data as Figure 2(a). The number of absorbers in A1 to A5 were 232, 229, 249, 225, and 189, respectively. B1 in (b) is showing the same data as Figure 2(b). The number of absorbers in B1 to B5 were 1087, 1113, 1057, 1085, and 1125, respectively. If the concentration is defined as the number of absorbers per unit volume, and each volume of in A1 to A5 and B1 to B5 is 1mm×0.55mm×0.16mm =0.088μL, then the concentration of absorbers in A1 to A5 are 2.6, 2.6, 2.8, 2.6, and 2.1 $\times 10^3/\mu L$, respectively, and the concentration of absorbers in B1 to B5 are 12.4, 12.6, 12.0, 12.3, and 12.8 $\times 10^3/\mu L$, respectively.

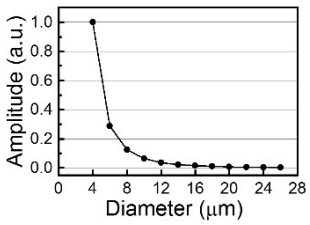

Fig. S3. Simulation results of the relationship between PA amplitude and hemoglobin distribution diameter. The results were simulated using the MATALAB K-wave tool, in which the amount of hemoglobin was set as constant and being distributed in a spherical apace. The variation of hemoglobin distribution diameter corresponds to the release process of hemoglobin after the rupture of an RBC. According to Ref [1] below, the mean volume of bovine RBCs is 41 μm^3, thus the initial hemoglobin distribution diameter was ~4.3 μm. The PA signal sensor was with a central frequency of 50 MHz and a bandwidth of 80.6%.

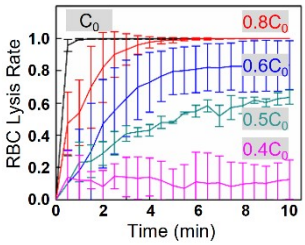

Fig. S4. Calibrated RBC lysis rate outside hydrogels in RBC lysis solution with different concentrations.

Reference:

1. I. T. Ivanov, B. K. Paarvanova, B. B. Tacheva and T. Slavov, *Gen. Physiol. Biophys.*, 2020, **39**, 505-518.